Vol 16 No 8, August 2007
1009-1963/2007/16(08)/2310-05

Chinese Physics

© 2007 Chin. Phys. Soc.
and IOP Publishing Ltd

Electronic structure and defect states of transition films from amorphous to microcrystalline silicon studied by surface photovoltage spectroscopy*

Yu Wei(于 威), Wang Chun-Sheng(王春生)†, Lu Wan-Bing(路万兵), He Jie(何 杰), Han Xiao-Xia(韩晓霞), and Fu Guang-Sheng(傅广生)

College of Physical Science and Technology, Hebei University, Baoding 071002, *China*

(Received 4 August 2006; revised manuscript received 12 December 2006)

In this paper, surface photovoltage spectroscopy (SPS) is used to determine the electronic structure of the hydrogenated transition Si films. All samples are prepared by using helicon wave plasma-enhanced chemical vapour deposition technique, the films exhibit a transition from the amorphous phase to the microcrystalline phase with increasing temperature. The film deposited at lower substrate temperature has the amorphous-like electronic structure with two types of dominant defect states corresponding to the occupied Si dangling bond states (D^0/D^-) and the empty Si dangling states (D^+). At higher substrate temperature, the crystallinity of the deposited films increases, while their band gap energy decreases. Meanwhile, two types of additional defect states is incorporate into the films as compared with the amorphous counterpart, which is attributed to the interface defect states between the microcrystalline Si grains and the amorphous matrix. The relative SPS intensity of these two kinds of defect states in samples deposited above 300°C increases first and decreases afterwards, which may be interpreted as a result of the competition between hydrogen release and crystalline grain size increment with increasing substrate temperature.

Keywords: microcrystalline silicon, defect states, surface photovoltaic spectroscopy
PACC: 0700, 7125W, 7155

1. Introduction

The hydrogenated transition films from amorphous (a-Si:H) to microcrystalline silicon (μc-Si:H) have attracted much attention because the most stable high-performance a-Si:H solar cells can be obtained just below the onset of microcrystallinity.[1,2] The presence of microcrystalline Si grains and reduced defects offer potential improvements in their solar energy conversion efficiency and carrier transport properties.[3,4] Considerable work has been concentrated on the deposition and characterization of a-Si:H transition films, though it is still a major subject to understand their nature and the connection between microstructures and optoelectronic properties.

Many techniques have been used to investigate the nature and optoelectronic properties of the a-Si:H transition films. The electronic density of states was analysed by photoluminescence, optical absorption and photocapacitance techniques.[5–7] The defect state distribution was determined by post-transit time-of-flight spectroscopy. The improvement of the device properties has been correlated to the improved structural order and the associated lower defect density in the films. However, few works have concentrated on directly determining the electronic structures and correlating them with the microstructures of transition a-Si:H films. Surface photovoltage spectroscopy (SPS) is a well-known surface-sensitive technique for studying the surface electronic structure of semiconductor materials and devices.[8–11] SPS measured the results that the change in surface potential due to optically excited electron–hole pair under periodic illumination and subsequent carrier redistribution or capture in the surface states, which can give the information about both the optical and electronic properties of semiconductor structures, e.g. band gap energies and gap states characteristics. It is nondestructive and more immediate and sensitive in comparison with optical absorption and the x-ray photoelectron spectroscopy technique. In this work, the characteristics of the band and defect states have been analysed by SPS technique for the a-Si:H transition films prepared by helicon wave plasma-enhanced

*Project supported by the Natural Foundation of Hebei province, People's Republic of China (Grant No 503129).
†Corresponding author. E-mail: whipug@163.com

chemical vapour deposition (HW-PECVD) method. Raman scattering analysis is used to identify the microstructures of the deposited films. Their band gaps and defect state distributions are obtained by SPS analysis. The variation of the distribution characteristics of defect states in the transition films with different microstructures has been discussed according to their growth conditions.

2. Experimental details

The a-Si:H and μc-Si:H samples are deposited on the substrates of the 7059 glass wafers with or without SnO_2 coating layer simultaneously by HW-PECVD technique, which has been discussed in detail elsewhere.[12] In the experiment, the SiH_4 and H_2 flow rate is kept at 2 sccm and 40 sccm respectively. The substrate temperature is used as a parameter to modify film crystallinity. The microstructure of the deposited films is characterized by Raman scattering spectroscopy, where an Ar^+ laser (514.5 nm) is used as an excitation source. The incident laser power on the samples is less than 1mW. The band gap energy is analysed through UV–Visible (UV–Vis) absorption measurements.

The surface photovoltage (SPV) technique is used to characterize the electronic structures and defect distribution of the deposited films. A 150W tungsten-halogen lamp through a prism monochrometer is used as a light source. The output light is periodically modulated and is focused on the sample in an area of 0.5 cm^2 through a set of lens. In the experiment, the capacitive coupling soft contact geometry is adopted to pickup the signal through an indium tin oxide (ITO) coated glass electrode above the sample.[13] The AC variation of the surface potentials vs light wavelength is recorded by a SR510 lock-in amplifier in phase with the modulated light.

3. Results and discussion

Figure 1 shows the Raman spectra of the films deposited on the glass wafer at different substrate temperatures. There are mainly three parts in all Raman spectra: (1) 100–200 cm^{-1}, the transverse acoustical (TA) vibration mode of amorphous silicon (a-Si); (2) 200–450 cm^{-1}, the longitudinal acoustical (LA) and longitudinal optical (LO) vibration mode of a-Si; (3) 450–550 cm^{-1}, the superposition of transverse optical (TO) vibration mode of a-Si and μc-Si:H. It can be seen that the intensities of TA, LA and TO mode peaks corresponding to a-Si decrease as temperature increases which suggests that the amorphous fraction decreases gradually when the substrate temperature increases. Normally the TO mode of a-Si is at 480 cm^{-1}, and that of single crystalline Si is at the 520 cm^{-1}. The scattering peak of the sample prepared under 200°C is at 490 cm^{-1} which suggests that the deposited film is more amorphous-like. The TO scattering peak shifts to higher wavenumber for the samples deposited at a higher substrate temperature, indicating that the crystallinity of the deposited films increases with increasing the substrate temperature. For 350°C and 400°C samples, a high-wavenumber shoulder peak around 510cm^{-1} appears, indicating that large μ-Si grains have formed in these transition films. In order to give the crystallinity of these films, we use a multi-Gaussian analysis to fit the Raman spectrum.[14] The film consists of a-Si matrix, μ-Si grain and an intermediate component. The microcrystalline volume fraction is obtained by the equation $X_c = (I_c + I_{GB})/(I_c + I_{GB} + I_a)$, where I_c, I_{GB} and I_a are integrated intensities of the μ-Si, intermediate and a-Si peaks respectively. The microcrystalline volume fractions of 33%, 48%, 50% and 55% are obtained for 200°C, 300°C, 350°C and 400°C samples respectively, where the fraction of the transition phase is more than 30% for all these films. There must be a large amount of grain boundary at surface of crystalline silicon grains for their difference microstructures from that of amorphous phase.

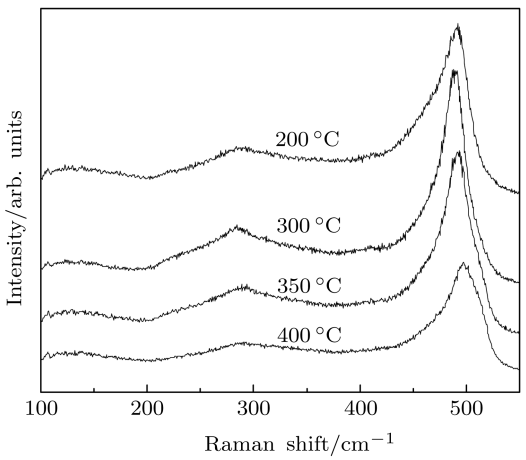


Fig.1. Raman spectra of samples deposited under the different substrate temperatures

The SPV measurement is performed on the films deposited on ITO coated glass substrate. A tangent

method is used, through which we can determine the position and type of the electronic states.[15] Under a sub-bandgap illumination, the dominant charge generation process is the exchange of charge carriers between the semiconductor bands and local states. Under super-bandgap illumination, the orders of magnitude of the probability of band-to-band absorption is typically larger than that of the probability of trap-to-band absorption and then the effect of trap-to-band absorption is negligible.

Figure 2(a) shows the SPS of the film deposited at the substrate temperature of 200 °C, in order to emphasize the changes in the slope of the SPS we add the extrapolated slopes to the figure. As can be seen, the main feature of the SPS is that its intensity goes through a slow increase at 2.15eV, which should be the response of band-to-band transition. It has been shown by Raman spectra that there is a low crystalline content in this sample. So the rise at 2.15 eV corresponds to the band gap of amorphous Si and this value is consistent with that determined by UV–Vis measurement as shown in Fig.2(b), where the optical band gap E_g is determined by $(\alpha h\nu) = (h\nu - E_g)^{1/2}$, where α is the absorption coefficient and $h\nu$ is the photon energy.[16] Besides the bandgap energy, there are some other SPS features as shown in the inset of Fig.1(a) about different kinds of defect states in the film. The fist positive slope developing at $h\nu = 1.05$ eV indicates an electronic excitation from a localized state into the conduction band which lies at $E_c - 1.05$ eV. The negative slope developing at $h\nu = 1.49$ eV corresponds to an electronic excitation from the valence band to a localized state which lies at E_v+1.49eV. Finally the negative slope change at $h\nu = 1.86$eV corresponds to the top of the valance band tail marked as $E_c - 1.86$ eV.

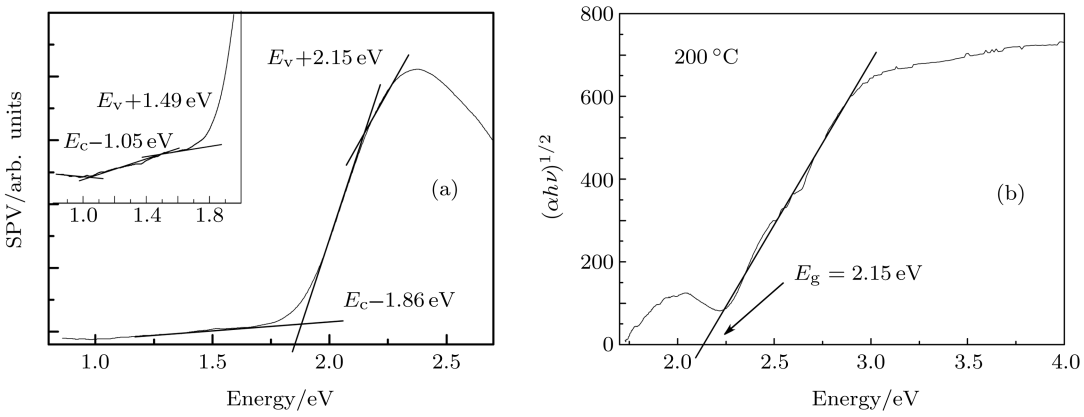


Fig.2. SPV and UV-VIS absorption spectra of samples deposited under 200 °C. (a) The SPV spectrum. (b) $(\alpha h\nu)^{1/2}$ against photon energy.

According to above analysis, the electronic band structures of this 200 °C deposited film is similar to undoped amorphous Si films deposited by PECVD technique.[17] Setting the valence band E_v as reference, we find that the top of valence band tail is at 0.29 eV above, which is calculated from the difference between the band gap and the top of valance band tail. Donor-like state of $E_c - 1.05$ eV is primarily occupied by electrons and it is ascribed to single or double occupied dangling band (D^0, D^-) and E_V+1.49eV is ascribed to singled or unoccupied dangling band (D^0, D^+) which is primarily positively charged.[18]

Figure 3 shows the SPS spectra of the samples deposited at higher substrate temperature. Parts of SPS characterizing the detailed distribution of gap states are given in every inset of the figure. As can be seen, the position of the SPS with a sharp increase is the characteristic of beginning of band-band absorption, which moves to lower energy than that of the 200 °C sample. The derived bandgaps are 2.14 eV, 1.96 eV and 1.92 eV for 300 °C , 350 °C and 400 °C samples respectively. The bandgap decreases with increasing the substrate temperature, this is consistent with the results of microcrystallinity improvement and the microcrystalline Si grain size increment.[19] The positive signals have been ensured by adjusting the phase of lock-in amplifier which has about 180° difference contrast with that in Fig.2, so each negative slope in these figures is attributed to a transition from the donor-like state occupied primarily by electrons to the conduc-

tion band and each positive slope change is identified as a transition from the valence band to the acceptor-like state, which is occupied by holes. Four defect states can be derived from these samples, which are shown in the insets of Fig.3. The positions of these defect states are listed in Table 1.

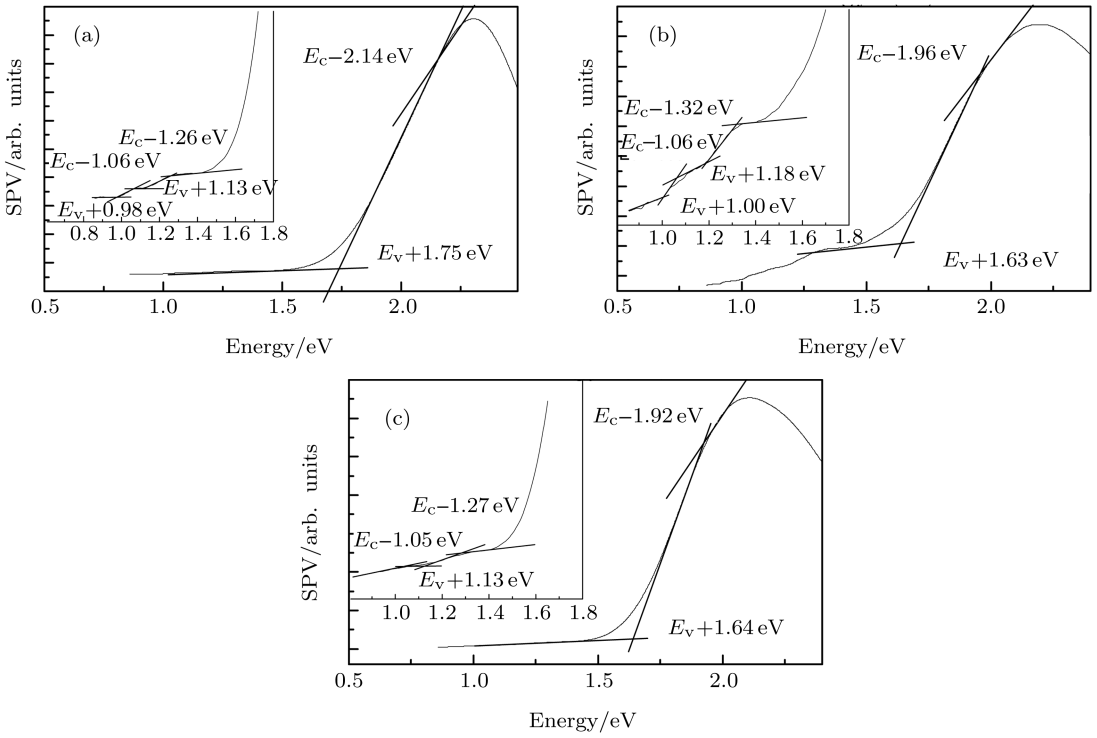


Fig.3. SPV spectra of the films deposited under different temperatures: (a) 300 °C, (b) 350 °C and (c) 400 °C.

Table 1. Position of defect states in the μc-Si:H films deposited under the different temperatures.

Deposited temperature	Position of acceptor-like states: $E_v + b_2$ and $E_v + b_1$		Position of donor-like states: $E_c - a_1$ and $E_c - a_2$	
300 °C	E_v+0.98eV	E_v+1.13eV	$E_c - 1.06$eV	$E_c - 1.26$V
350 °C	E_v+1.00eV	E_v+1.18eV	$E_c - 1.06$eV	$E_c - 1.32$V
400 °C		E_v+1.13eV	$E_c - 1.05$eV	$E_c - 1.27$V

The electronic structure and the distribution of defect states in μc-Si:H films postulated from the above SPS measurements can be schematically shown in Fig.4. The defect states in the band gap have split into four groups which are signified as $E_c - a_1$, $E_c - a_2$, $E_v + b_1$, $E_v + b_2$ in the diagram. This splitting comes from the incorporation of more microcrystalline Si grains into μc-Si:H films in comparison with the amorphous-like film. From Table 1 and the insets in Fig.3 we can see that the location of these states has changed only a little. Besides, the $E_c - a_2$ and $E_v + b_2$ states are deeper states and have a larger intensity change in SPS in comparison with the $E_c - a_1$ and $E_v + b_1$ states, which can be tentatively interpreted as follows: that these two defect states are contributed to the Si dangling band in amorphous Si matrix and the other two defect states $E_c - a_1$ and $E_v + b_1$ are contributed to dangling bands at the interface between microcrystalline Si and the amorphous matrix.[20] This is also consistent with the three-phase model, which suggests that μc-Si:H consists of crystalline grains surrounded by grain boundaries and embedded in an amorphous matrix,[21] in this case, the defect absorption from the disordered grain boundaries (GB) becomes evident.[22] The intensity variation of the SPS concerning the defect states at different substrate temperatures is

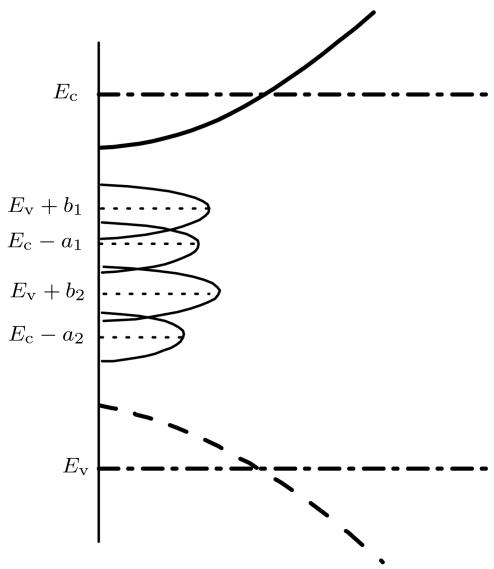


Fig.4. Schematic diagram of electronic structure and distribution of defect states in microcrystalline Si films.

closely related with the microstructure change. As can be seen in Fig.3, the relative SPS intensity of defect states to that of band-band transition increases first and decreases later with increasing deposition temperature and the $E_v + b_2$ state becomes ambitious for 400 °C sample. This trend can be accounted for by the competition between hydrogen releasing effect and Si grain size increasing while the films grow. With the increasing substrate temperature, the density of silicon dangling bonds at the surface of microcrystalline Si grains and in amorphous Si matrix will increase because of the enhanced possibility of bonded hydrogen releasing, which is the cause of SPS signal enlargement. While both the crystallinity and the size of nanocrystalline Si particles increasing at a higher substrate temperature will change the above tendency, the reduction of amorphous contents and GB areas causes a decline of the density of Si dangling bonds at the interface and in the amorphous matrix and then the decrease of SPS intensity.

4. Conclusion

In summary, the SPS technique has been used to characterize the defect states of hydrogenated amorphous and microcrystalline Si films. The analysis shows that there are two defect states in amorphous-like Si, which can be attributed to the unoccupied, single occupied and double occupied dangling band. For microcrystalline Si, there are two additional defect states, correlated to the interface states between microcrystalline Si grains and amorphous matrix; the position of these states only have a small shift. The relative intensity of these two kinds of defect states in samples deposited above 300 °C increases first and decreases afterwards due to the competition effect of hydrogen release and crystalline grain size increment with increasing substrate temperature.

References

[1] Guha S, Yang J and Williamson D L 1999 *Appl. Phys. Lett.* **74** 1860

[2] Lei Q S, Wu Z M, G X H, Zhao Y, Sun J and Xi J P 2006 *Chin. Phys.* **15** 3033

[3] Sheng S, Liao X and Kong G 2001 *Appl. Phys. Lett.* **78** 2509

[4] Shi J J, Huang S Y, Chen K J, Huang X F and Xu J 2001 *Chin. Phys.* **10** 748

[5] Yue G, Lorentzen J D, Lin J, Wang Q and Han D 1999 *Appl. Phys. Lett.* **75** 492

[6] Han D, Yue G, Lorentzen J D, Lin J, Habuchi H and Wang Q 2000 *J. Appl. Phys.* **87** 1882

[7] Guha S, Yang J and Williamson D L 1999 *Appl. Phys. Lett.* **74** 1860

[8] Balestra C L, Lagowski J and Gatos H C 1971 *Surf. Sci.* **26** 317

[9] Gatos C L and Lagowski J 1973 *J. Vac. Sci. Technol.* **10** 130

[10] Burstein L, Shapira Y, Moons E and Cahen D 1994 *Appl. Surf. Sci.* **74** 201

[11] Leibovitch L, Kronik L, Fefer E and Shapira Y 1994 *Phys. Rev.* **50** 1739

[12] Yu W, Liu L H and Hou H H 2003 *Acta Phys. Sin.* **52** 687

[13] Sharma T K, Porwal S, Kumar R and Shailendra Kumar 2001 *Rev. Sci. Instrum.* **73** 1835

[14] Han D, Lorentzen J D, Weinberg-Wolf J and McNeil L E 2003 *J. Appl. Phys.* **94** 2930

[15] Burstein L, Shapira Y, Partee J, Shinar J, Lubianiker Y and Balberg I 1997 *Phys. Rev.* B **55** 1930

[16] Park Y B, Li X, Rhee S W and Park D W 1999 *J. Phys. D: Appl. Phys.* **32** 1955

[17] Mensing G, Gilligan J, Hari P, Hurt E, Tolk N and Taylor P C 2002 *J. Non-Cryst. Solids* **299-302** 621

[18] Fefer E and Shapira Y 1995 *Appl. Phys. Lett.* **67** 371

[19] Matsumoto T, Suzuki J, Ohmura M, Kanemitsu Y and Masumoto Y 2001 *Phys. Rev.* B **63** 195322

[20] Reynolds S, Smirnov V, Main C, Carius R and Finger F 2003 *MRS Symp. Proc.* **762** A4.3.1

[21] Diehl F, Scheib M, Schroder B and Oechsner H 1998 *J. Non-Cryst. Solids* **227-230** 973

[22] Jackson W B, Johnson N M and Biegelsen D K 1983 *Appl. Phys. Lett.* **43** 195